Improved Human Erythropoiesis and Platelet Formation in Humanized NSGW41 Mice

Susann Rahmig,[1] Romy Kronstein-Wiedemann,[2,3] Juliane Fohgrub,[1] Nicole Kronstein,[2,3] Aleksandra Nevmerzhitskaya,[1,6] Martin Bornhäuser,[3] Max Gassmann,[4] Alexander Platz,[5] Rainer Ordemann,[3] Torsten Tonn,[2,3] and Claudia Waskow[1,*]

[1]Regeneration in Hematopoiesis and Animal Models in Hematopoiesis, Institute for Immunology, Medical Faculty Carl Gustav Carus, Technische Universität Dresden, Fetscherstrasse 74, 01307 Dresden, Germany
[2]Institute for Transfusion Medicine, German Red Cross Blood Donation Service North-East, 01307 Dresden, Germany
[3]Universitätsklinikum Carl Gustav Carus der TU Dresden, Medizinische Klinik und Poliklinik I, 01307 Dresden, Germany
[4]Institute of Veterinary Physiology, Vetsuisse Faculty and Zurich Center for Integrative Human Physiology (ZIHP), University of Zurich, 8057 Zurich, Switzerland
[5]DKMS Cord Blood Bank, Enderstrasse 94, 01277 Dresden, Germany
[6]Present address: Georg-Speyer-Haus, Institute for Tumor Biology and Experimental Therapy, 60596 Frankfurt, Germany
*Correspondence: claudia.waskow@tu-dresden.de
 http://dx.doi.org/10.1016/j.stemcr.2016.08.005

SUMMARY

Human erythro-megakaryopoiesis does not occur in humanized mouse models, preventing the in vivo analysis of human hematopoietic stem cell (HSC) differentiation into these lineages in a surrogate host. Here we show that stably engrafted KIT-deficient NOD/SCID $Il2rg^{-/-} Kit^{W41/W41}$ (NSGW41) mice support much improved human erythropoiesis and platelet formation compared with irradiated NSG recipients. Considerable numbers of human erythroblasts and mature thrombocytes are present in the bone marrow and blood, respectively. Morphology, composition, and enucleation capacity of de novo generated human erythroblasts in NSGW41 mice are comparable with those in human bone marrow. Overexpression of human erythropoietin showed no further improvement in human erythrocyte output, but depletion of macrophages led to the appearance of human erythrocytes in the blood. Human erythropoiesis up to normoblasts and platelet formation is fully supported in NSGW41 mice, allowing the analysis of human HSC differentiation into these lineages, the exploration of certain pathophysiologies, and the evaluation of gene therapeutic approaches.

INTRODUCTION

Erythrocytes are essential for oxygen supply, and anemia can have severe systemic consequences. The causes of anemia include iron deficiency/blood loss, cancer, infectious disease, and genetic disorders such as sickle cell anemia or thalassemia. Analysis of mechanisms leading to anemia is severely limited by the lack of appropriate in vivo models (Pishesha et al., 2014). Also, the generation of functional platelets in humanized mouse models is challenging. Abnormal platelet generation and function cause bleeding disorders and evoke thrombotic and cardiovascular diseases that are potential causes of mortality (Massberg et al., 2002). To date, the ex vivo generation of platelets from donor-independent or autologous sources has been hampered by an incomplete understanding of mechanisms promoting platelet differentiation and maturation (Karagiannis and Eto, 2015; Lambert et al., 2013). Finally, it is impossible to test for differentiation of these lineages in vivo (Mende et al., 2016), underlining the need for suitable in vivo models to study these processes.

Many immunodeficient mouse models receptive for transplantation of human hematopoietic stem cells (HSCs) have been developed over the last decade to support the engraftment and differentiation of specific hematopoietic lineages (Cosgun et al., 2014; Chen et al., 2009; Rongvaux et al., 2014). However, in all mouse models available to date human erythropoiesis is severely impaired. In contrast, human platelets can develop and mature in humanized mouse models, but their output is generally very low (Hu and Yang, 2012; Rongvaux et al., 2011; Suzuki et al., 2007). Clearance of human red blood cells (RBCs) by macrophages after infusion into CD47-deficient mice suggests that absence of RBCs and their immediate progenitors is due to signal-regulatory protein alpha (SIRPalpha)-independent phagocytic activity (Hu et al., 2011). Furthermore, macrophage depletion or overexpression of human interleukin-3 (IL-3) and human erythropoietin (hEPO) lead to the transient appearance of low numbers of human RBCs in the blood of humanized mice (Hu et al., 2011; Chen et al., 2009). Also, thrombocyte reconstitution in the blood can be further improved by treatment with clodronate liposomes or pegylated recombinant human megakaryocyte growth and development factor (Hu and Yang, 2012; Suzuki et al., 2007). However, due to the transient nature of the increase of human RBCs and human platelets in all models, the use of humanized mouse models to study human erythrocyte differentiation is severely limited.

We generated mouse strains suitable for humanization by introducing loss-of-function KIT receptors (W41 or Wv alleles) into NOD/SCID $Il2rg^{-/-}$ (NSG; NSGW41, NSGWv) or BALB/c $Rag2^{-/-} Il2rg^{-/-}$ (BRgWv) mice (Cosgun et al.,
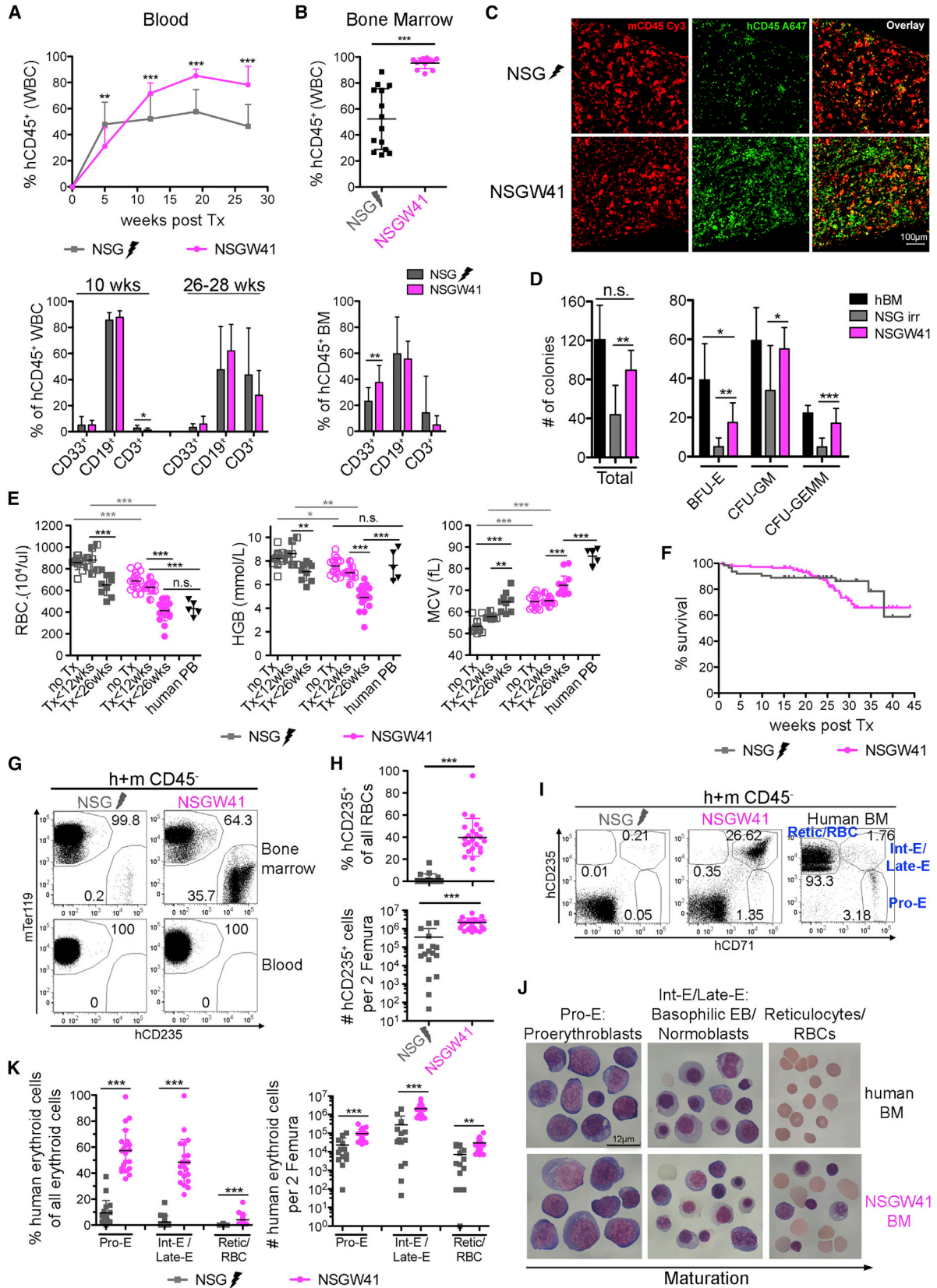
(legend on next page)

2014). These mice efficiently support stable engraftment of human hematopoietic stem and progenitor cells (HSPCs) in the long term without the need for previous conditioning therapy, and were instrumental for the study of effects of cell physiological processes on human HSC function in vivo (Mende et al., 2015). A second striking feature is the remarkably increased engraftment of human myeloid cells in bone marrow (BM) and spleen, evidencing that stable stem cell engraftment is sufficient to ensure continuous output of human myeloid cells (Cosgun et al., 2014; Rahmig et al., 2015). In BRgWv mice, low frequencies of human erythroid cells were detected in the BM (Cosgun et al., 2014), suggesting that RBC generation may occur in humanized KIT-mutant recipient mice. Here, we show the efficient differentiation of human donor HSPCs into erythroblasts/normoblasts and megakaryocytes in humanized NSGW41 recipients compared with conventional NSG recipients, suggesting that growth factors responsible for these differentiation paths are compatible across species. Mature human RBCs are absent and low numbers of human platelets are found in the blood, but macrophage depletion transiently restores erythrocyte and platelet repopulation. The entire differentiation from human HSCs into RBCs and platelets is recapitulated in the murine BM, providing an in vivo setting that allows for the study of the regulation of RBC and platelet formation in health and disease.

RESULTS AND DISCUSSION

Human Erythropoiesis in NSGW41 Recipients

Transplantation of human CD34-enriched cord blood (CB) cells results in enhanced and uniform engraftment of human leukocytes in the blood (Figure 1A) and BM (Figures 1B and 1C) of NSGW41 recipients compared with irradiated NSG mice. Colony formation confirmed the presence of increased numbers of lineage-specific progenitors in humanized NSGW41 mice compared with controls (Figure 1D), evidencing improved engraftment of human HSPCs. To test whether cell-intrinsic impairment of murine erythropoiesis (Sharma et al., 2007) provides an advantage for human RBC differentiation, we compared blood cell parameters between non-transplanted and humanized mice (Figure 1E). Non-transplanted NSGW41 mice display a macrocytic anemia (Sharma et al., 2007). After humanization, RBC parameters decreased in both recipients but were more pronounced in NSGW41 mice. Despite the severe anemia in NSGW41 mice, the survival between both humanized mouse strains was comparable (Figure 1F). Neither conditioned NSG nor unconditioned NSGW41 mice showed human RBCs in the circulation (Figure 1G). In contrast, the BM of NSGW41 mice was highly repopulated with human erythroid progenitor cells (Figures 1G and 1H) that were present only at low frequencies in the donor cells (Figure S1D), suggesting that stable human HSC engraftment supports an increased output of cells of the erythroid lineage. Consistent with this interpretation is the fact that the transplantation of sorter-purified human HSCs also results in the engraftment of human erythroblasts in the BM of KIT-mutant recipient mice (Koichi Akashi, personal communication).

To assess for a specific block of differentiation due to a potential incompatibility for human RBC differentiation in the murine environment, we quantified erythroid precursors (pro-E, Int-E/Late-E, Retic/RBC, Figures 1I and 1J). All differentiation stages were present, and increased numbers of human RBC progenitors were detected in humanized NSGW41 compared with NSG recipients (Figures S1C and 1K), suggesting that human erythropoiesis is strongly

Figure 1. Improved Human Erythroid Engraftment in NSGW41 Mice
(A and B) Human leukocyte chimerism (top) and composition of human graft (bottom): (A) in the blood at indicated time points, five experiments, 2–5 mice per experiment; and (B) in the BM of NSG and NSGW41 recipients 24–32 weeks after humanization, five experiments, 2–4 mice per experiment.
(C) Immunofluorescence of human and mouse CD45^{+} cells in bone sections of NSG and NSGW41 recipients. Scale bar, 100 μm.
(D) Colony assays. Two experiments, 2–5 mice per experiment, two technical replicates each.
(E) Blood parameters of non-transplanted (open) and transplanted NSG and NSGW41 mice early (<12 weeks, half-filled) and late (>26 weeks, closed) after humanization. There is no discrimination between human and mouse parameters. Five experiments, 2–8 mice per experiment.
(F) Survival plot after humanization. Twenty experiments, 3–16 mice per experiment.
(G) RBC chimerism.
(H) Frequency (top) and number per two femura (bottom) of CD235^{+} cells within all erythrocytes. Seven experiments, 2–9 mice per experiment.
(I) Human erythroid precursors.
(J) Giemsa-stained cells sorted as shown in (I). Scale bar, 12 μm.
(K) Frequencies (left) and numbers (right) of cells of human origin within all erythroid cells of the indicated differentiation stage in humanized mice. Seven experiments, 2–9 mice per experiment.
Data represent means ± SD. *p = 0.05–0.01, **p = 0.01–0.001, ***p < 0.001; n.s., not significant. See also Figure S1.
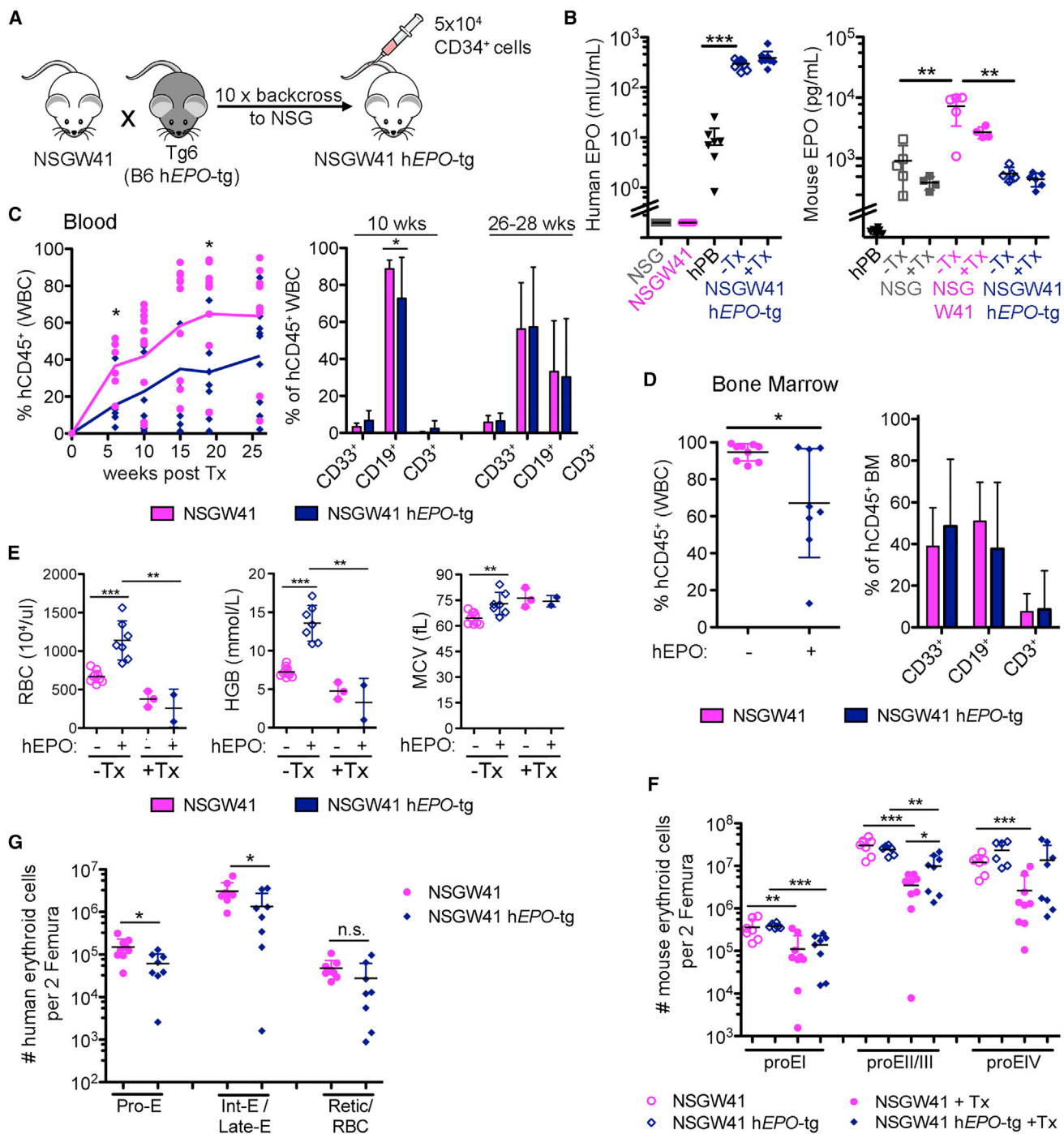
Figure 2. Overexpression of Human Erythropoietin in NSGW41 Mice

(A) Generation of NSGW41 h*EPO*-tg mice.

(B) Human (left) and murine (right) blood EPO levels in indicated mice and human controls (hPB). human EPO: two experiments, 3–6 replicates each; mouse EPO: one experiment, 4–6 replicates each.

(C) Human leukocyte chimerism (left) and donor cell composition in the blood (right). Four experiments, 2–4 mice per experiment.

(D) BM leukocyte chimerism (left) and graft composition (right) 25–32 weeks after humanization. Four experiments, 1–3 mice per experiment.

(legend continued on next page)

supported in NSGW41 mice. Engraftment of human erythroblasts/normoblasts in NSGW41 occurred at the expense of endogenous erythroid progenitors (Figures S1A and S1B), resulting in a more pronounced anemia in NSGW41 mice. We conclude that stable human HSC engraftment is a prerequisite for continuous human erythropoiesis in mice, and commitment to the erythroid lineage and differentiation up to nucleated erythroid progenitor stages is supported by the murine microenvironment in NSGW41 recipients.

Overexpression of Human Erythropoietin Fails to Enhance Human RBC Engraftment

The injection of h*EPO*- and *IL-3*-encoding plasmids into humanized NSG mice results in the appearance of low frequencies of human CD235$^+$ erythrocytes in the blood (Chen et al., 2009). To test whether the overexpression of hEPO (Waskow et al., 2002, 2004) in NSGW41 mice increases RBC reconstitution, we generated NSGW41 h*EPO*-transgenic (h*EPO*-tg) mice (Figure 2A). Increased plasma hEPO levels were confirmed before and after humanization (Figure 2B). NSGW41 mice, comparable with *Kit* mutants in other genetic backgrounds (Waskow et al., 2004), displayed 8-fold higher mouse EPO levels in response to the endogenous anemia (Geissler et al., 1981). hEPO levels in NSGW41 h*EPO*-tg mice were ~50-fold elevated compared with human blood. Human donor cell chimerism was reduced in the blood and BM of NSGW41 h*EPO*-tg mice compared with NSGW41 mice (Figures 2C and 2D), suggesting that hEPO induces differentiation of donor HSPCs and prevents their efficient engraftment. However, hEPO had no effect on the composition of human white blood cells (Figures 2C and 2D). RBC parameters were significantly increased in non-transplanted NSGW41 h*EPO*-tg mice, evidencing the functionality of the surplus hEPO, but after humanization RBC counts and hemoglobin contents still significantly decreased in both mouse strains (Figure 2E). The number of murine erythroblasts/normoblasts decreased equally in humanized NSGW41 h*EPO*-tg or NSGW41 mice (Figures 2F and S1B). Regardless, the engraftment of human erythroblasts in BM of humanized NGSW41 h*EPO*-tg mice was reduced compared with NSGW41 mice (Figure 2G) and no mature human RBCs were found in the blood of recipients. This evidences a lack of support for human erythroid engraftment by hEPO overexpression. EPO supports RBC differentiation in mice and humans at late stages during erythroid differentiation by promoting erythroblast proliferation and inhibiting apoptosis (Kaushansky, 2006; Waskow et al., 2004). However, intermediate and late stages of erythroid differentiation are particularly well repopulated by cells of human origin in NSGW41 mice (Figures 1G–1K), suggesting a defect at or beyond the enucleation of human RBC precursors.

Depletion of Macrophages Partially Rescues Erythrocyte Maturation

Phagocytosis has been considered an alternative cause for lack of human RBCs in humanized mice (Hu et al., 2011). Endogenous murine macrophages are reduced after humanization (Figure S2A) but remain phagocytically active (Figure S2B). To deplete macrophages we injected clodronate-containing liposomes (CloLip) (Figure 3A), which cleared phagocytes from the blood ((Hu et al., 2011), Figures 3B and 3C) and resulted in the appearance of human RBCs in the circulation of humanized NSGW41 mice (Figures 3B and 3D). Correspondingly, the composition of human BM erythroid cells was altered and the frequency of Int-E/Late-E cells (CD71$^+$ CD235$^+$) was significantly reduced, whereas CD235$^+$ Retic/RBCs increased (Figure 3E). We conclude that the depletion of macrophages improves human erythrocyte reconstitution in the blood of humanized mice but the shift toward more mature erythroid cells is incomplete, perhaps due to a block within Int-E/Late-E erythroblasts/normoblasts that contain terminal differentiation stages prior to enucleation, or insufficient enucleation.

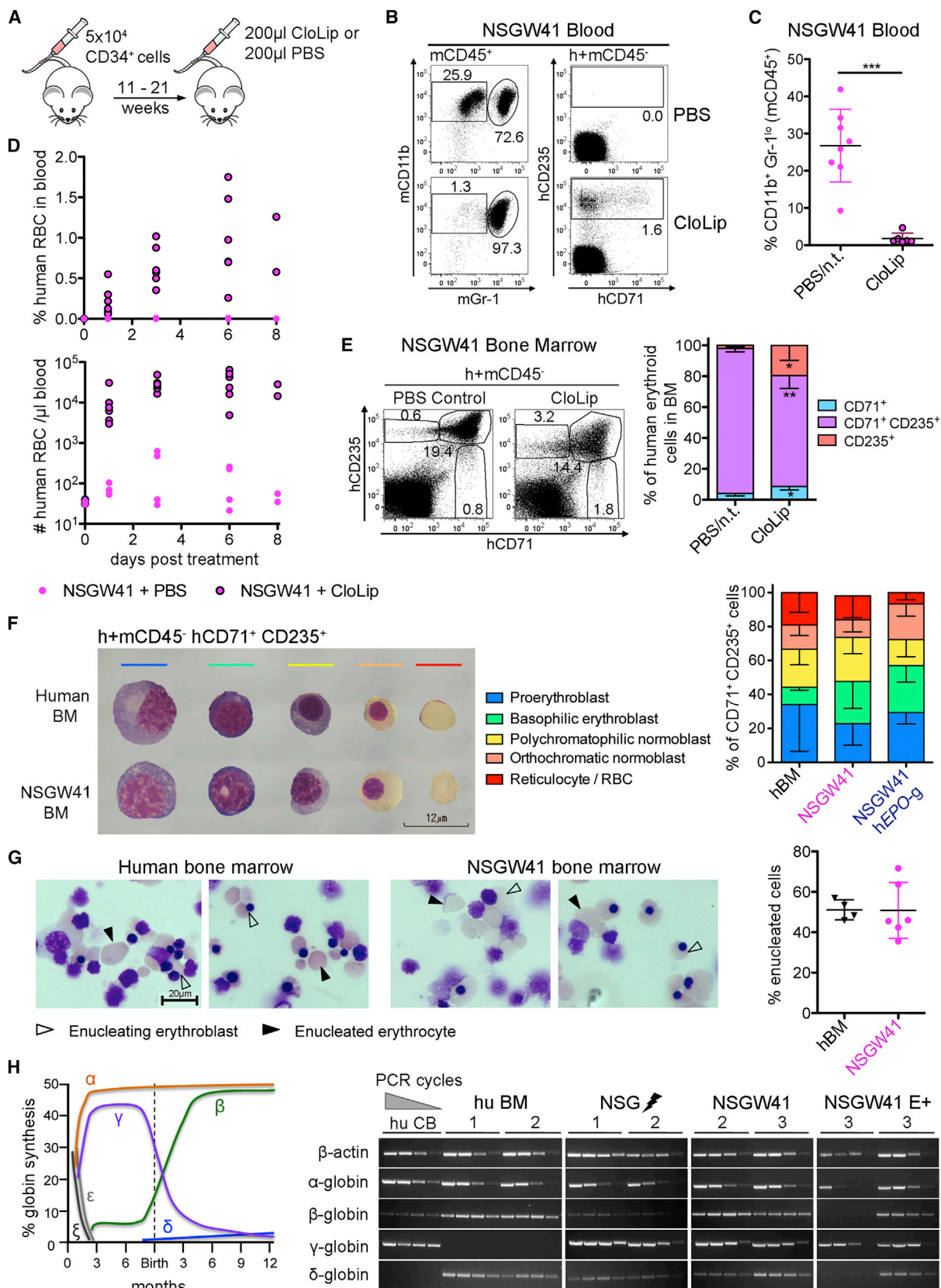### Human Erythroblasts Generated in NSGW41 Mice Can Terminally Differentiate

The composition of CD71$^+$ CD235$^+$ progenitors that contain pro- and basophilic erythroblasts, polychromatophilic and orthochromatic normoblasts, and reticulocytes was comparable between humanized NSGW41, NSGW41 h*EPO*-tg, and human BM (Figure 3F), evidencing normal erythroid differentiation in our mouse strains. Furthermore, human CD71$^+$ CD235$^+$ Int-E/Late-E erythroblasts from human or NSGW41 BM enucleated at comparable frequencies (Figure 3G), suggesting that human erythroblasts generated in mice can efficiently enucleate. However, we cannot formally exclude that the enucleation frequency in vivo differs between humanized mice and human BM because the formation of erythroblastic islands may require factors that are incompatible between the species (Dzierzak

(E) Blood parameters in NSGW41 and NSGW41 h*EPO*-tg mice with (31 weeks, one experiment, 2–3 mice) and without humanization (7–10 mice).

(F) Mouse RBC precursors per two femura. Four experiments, 1–3 mice per experiment.

(G) Human RBC precursors per two femura. Four experiments, 1–3 mice per experiment.

Data represent means ± SD. *p = 0.05–0.01, **p = 0.01–0.001, ***p < 0.001; n.s., not significant.

A 5×10⁴ CD34⁺ cells / 11 – 21 weeks / 200μl CloLip or 200μl PBS

B NSGW41 Blood

C NSGW41 Blood

D

E NSGW41 Bone Marrow

% of human erythroid cells in BM

CD71⁺
CD71⁺ CD235⁺
CD235⁺

● NSGW41 + PBS   ● NSGW41 + CloLip

F h+mCD45⁻ hCD71⁺ CD235⁺

Human BM

NSGW41 BM

Proerythroblast
Basophilic erythroblast
Polychromatophilic normoblast
Orthochromatic normoblast
Reticulocyte / RBC

% of CD71⁺ CD235⁺ cells

G Human bone marrow   NSGW41 bone marrow

▷ Enucleating erythroblast   ▶ Enucleated erythrocyte

H

PCR cycles

β-actin
α-globin
β-globin
γ-globin
δ-globin

(legend on next page)

and Philipsen, 2013). Adult globin chain gene expression was detected in CD71$^+$ CD235$^+$ cells from humanized mice, but the majority of transcripts encoded for fetal hemoglobin subunits (γ-globin) in all humanized mice (Figure 3H). However, humanized NSGW41 mice expressed increased amounts of transcripts encoding for adult-type β-globin. Furthermore, δ-globin, which is part of adult HbA2 hemoglobin, was not expressed in human CB but in all humanized mice, evidencing a globin switch in CB-derived erythroblasts. However, while silencing of γ-globin is not observed, β-globin activation seems to occur, suggesting that a globin switch is at least partially realized in humanized mice (Bauer and Orkin, 2011). The expression of fetal globin should not pose a problem to the final maturation and functionality of human erythrocytes in mice, as patients with a certain type of hereditary persistence of fetal hemoglobin who have 100% fetal hemoglobin display no anemia (Bauer and Orkin, 2011). We conclude that there is no block in human erythrocyte maturation in NSGW41 mice and assign paucity of human RBCs to either insufficient in vivo enucleation or SIRPalpha-independent phagocytosis.

Human Platelet Formation Is Improved in NSGW41 Mice

The reconstitution of human thrombocytes is severely impaired in humanized mouse models (Hu and Yang, 2012; Rongvaux et al., 2011; Suzuki et al., 2007). Non-transplanted NSGW41 mice display thrombocytopenia (Figure 4A). After transplantation thrombocytes decreased in irradiated NSG and NSGW41 mice, but the decline was accelerated and more severe in NSGW41 mice. After humanization, mature human megakaryocytes were present in NSGW41 and NSG mice (Figure 4B), but the frequency was much improved in NSGW41 compared with NSG recipients (Figure 4D). Consistently, hCD61$^+$ platelets were present in higher frequencies in BM and blood of humanized NSGW41 mice (Figures 4C and 4D). Despite a signifi-

cant improvement of human thrombocyte reconstitution in NSGW41 mice, the frequency of circulating platelets was still low compared with overall human chimerism (Figure 1A). Macrophage depletion resulted in an increase of human platelets in the blood (Figure 4E). Quantification of thrombocytes in the BM showed no difference between macrophage-depleted and control mice (Figure S3), suggesting that megakaryocyte/thrombocyte lineage commitment and maturation were not affected by macrophage depletion but that survival in the periphery was enhanced. We conclude that maturation and survival of human thrombocytes are increased in NSGW41 mice compared with irradiated NSG mice.

Our results show that stable human HSC engraftment is sufficient to support the generation and maturation of human erythrocytes, thrombocytes, and other myeloid cells (Cosgun et al., 2014). The increased engraftment of human cells in NSGW41 mice occurs at the expense of murine erythroblasts and megakaryocytes, suggesting replacement of endogenous hematopoiesis. We conclude that NSGW41 mice are an improved tool for the study of human erythrocytes and RBC-associated diseases. Despite the presence of high numbers of human erythroblasts/normoblasts in the BM of NSGW41 mice, we could only detect human erythrocytes in the circulation after macrophage depletion. Significant differences between human and mouse erythropoiesis were reported (An et al., 2014; Pishesha et al., 2014) but direct comparisons are difficult, as murine erythroblasts are usually isolated from BM whereas human erythroblasts are derived from in vitro culture of CD34$^+$ cells (Palis, 2014). We show here that there is no differentiation defect in the newly generated human erythroblasts, enucleation can take place, and even a partial globin chain switch occurs in mice, suggesting that growth factors important in RBC differentiation are cross-reactive between humans and mice. We reason that the murine NSGW41 environment enables human erythrocyte and thrombocyte differentiation

Figure 3. Terminal Erythroid Differentiation Is Not Impaired in Erythroblasts Generated in Mice
(A) Scheme of macrophage depletion by CloLip 11 to 21 weeks after humanization.
(B) Representative pictures of macrophage depletion.
(C) Frequencies of murine CD11b$^+$ Gr-1^{lo} macrophages in the blood of humanized NSGW41 mice that have received CloLip 24 hr before. n.t., not treated. Two experiments, 2–4 mice per experiment.
(D) Frequencies (top) and numbers (bottom) of human CD235$^+$ cells in the blood. Two experiments, 2–4 mice per experiment.
(E) Human BM erythroblasts/normoblasts 6–8 days after CloLip. One experiment, four mice.
(F) Giemsa-stained human RBC maturation stages within hCD71$^+$ CD235$^+$ cells. Composition of hCD71$^+$ CD235$^+$ cells in human BM (n = 3), BM from humanized NSGW41 mice (n = 5), and NSGW41 h*EPO*-tg mice (n = 3). Two experiments, ~110 cells counted on each cytospin.
(G) In vitro enucleation assay. Pictures from hCD71$^+$ CD235$^+$ erythroid cells after 7 days of culture. Scale bar, 20 μm. Right: quantification of enucleated cells, 162–248 cells per cytospin counted. Three experiments, 1–2 replicates per experiment.
(H) Scheme of human globin expression during development. Semi-quantitative analysis of human globin mRNA expression in sorted hCD71$^+$ CD235$^+$ cells.
Data represent means ± SD. *p = 0.05–0.01, **p = 0.01–0.001, ***p < 0.001. See also Figure S2.
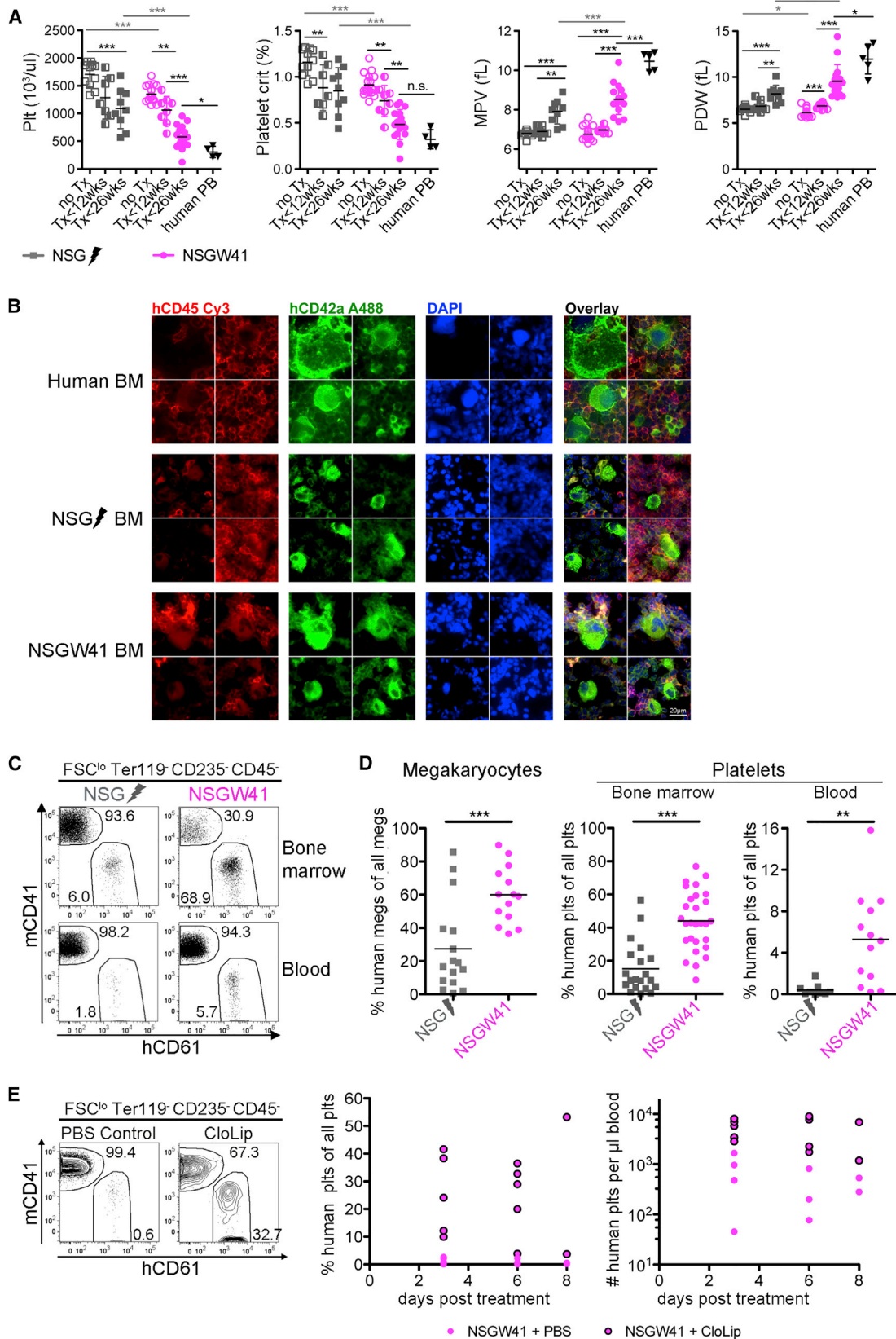
(legend on next page)

without additional manipulation, allowing for the in vivo analysis of human erythropoiesis.

EXPERIMENTAL PROCEDURES

Mice

NOD.Cg-*Prkdc*^{scid} *Il2rg*^{tm1Wjl}/SzJ mice (NSG) were obtained from the Jackson Laboratory. NOD.Cg-*Prkdc*^{scid} *Il2rg*^{tm1Wjl}/SzJ *Kit*$^{W41/W41}$ mice (NSGW41) were generated as previously described (Cosgun et al., 2014). To generate NSGW41 h*EPO*-tg mice, we backcrossed Tg6 mice (C57BL/6), which constitutively overexpress hEPO in a hypoxia-independent manner and show hematocrit values of up to 80% (Vogel and Gassmann, 2011), ten times onto NSG. Subsequently, NSG h*EPO*-tg mice were crossed with NSGW41 animals. All mice were bred and maintained under specific pathogen-free conditions at the animal facility of the TU Dresden. Animal experiments were performed in accordance with German animal welfare legislation and approved by the relevant authorities (Landesdirektion Dresden, Referat 24).

Human Donor Cells

Human umbilical CB samples were provided by the DKMS Cord Blood Bank, Dresden. Human BM samples were obtained from healthy BM donors in the Department of Hematology/Oncology of the University Hospital, Dresden. All human samples were used in accordance with the guidelines approved by the Ethics Committee of the Dresden University of Technology.

Transplantations

CD34$^+$ progenitor cells were isolated from human CB as described previously (Cosgun et al., 2014). For humanization 5 × 10^4 CD34-enriched cells were injected intravenously in 150 μL of PBS/5% fetal calf serum into 4- to 12-week-old conditioned NSG (200 cGy; MaxiShot, Yxlon) or unconditioned NSGW41 or NSGW41 h*EPO*-tg mice. After transplantation, mice were given neomycin-containing drinking water for 3 weeks.

Blood Analysis

For complete blood counts, blood of mice was collected in EDTA-containing microtubes. Blood samples were diluted in a ratio of 1:5 with NaCl 0.9% and analyzed on a Sysmex XT2000iV or Sysmex XE-5000 blood analyzer.

Flow Cytometry and Cell Sorting

BM and blood samples were collected and prepared as described previously (Cosgun et al., 2014). Samples were acquired on an LSRII cytometer (BD Biosciences) or a MACS Quant Analyzer (Miltenyi) and analyzed using FlowJo software (TreeStar). Sorting of human erythrocyte populations was performed on a FACSAria II or III (BD Biosciences). For determining total cell numbers, a specific volume of the respective cell suspension was analyzed on a MACS Quant Analyzer. Details regarding antibodies can be found in Supplemental Experimental Procedures.

Colony Assay

Human CD45$^+$ cells (5 × 10^4) were sorted from BM of humanized NSG and NSGW41 mice or fresh human BM samples and plated in duplicate into a 6-well plate with methylcellulose-containing medium supplemented with rhSCF, rhGM-CSF, rhG-CSF, rhIL-3, and rhEPO (MethoCult GF H84434; STEMCELL Technologies). After 14 days the number and types of colonies was analyzed using a STEMvision instrument (STEMCELL).

Enucleation Assay

Sorter-purified hCD71$^+$ CD235$^+$ BM cells (4.8 × 10^5 to 1 × 10^6) from humanized NSGW41 mice or fresh human BM samples were seeded in 1 mL of Iscove's modified Dulbecco's medium supplemented with 1% L-glutamine, 100 U/mL penicillin, 100 μg/mL streptomycin, 330 μg/mL holo-human transferrin, 10 μg/mL recombinant human insulin, 2 IU/mL heparin, and 5% pooled AB serum (German Red Cross Blood Donation Service North-East), and 3 U/mL human erythropoietin into 24-well plates (Giarratana et al., 2011). Medium was renewed after 3 days. On day 7 cells were collected, and 2 × 10^5 to 5 × 10^5 cells were cytospun and analyzed.

Morphological Analysis

Sorted BM or cultured cells were cytospun onto polylysine-coated slides at 25–100 × *g* for 5 min and after ON drying stained with May-Gruenwald-Giemsa. Photographs were taken using Nikon Eclipse TS100 or Keyence BZ9000 microscopes.

Macrophage Depletion

Macrophages were depleted by intravenous injection of 200 μL of clodronate liposomes (ClodronateLiposomes.com). Controls received 200 μL of PBS. Macrophage depletion was confirmed

---

Figure 4. Human Thrombopoiesis in NSGW41 Mice

(A) Blood parameters of NSG and NSGW41 mice with and without humanization. Plt, platelet; MPV, mean platelet volume; PDW, platelet distribution width. No discrimination between human and mouse parameters. Five experiments, 2–8 mice per experiment.

(B) Immunofluorescence of human megakaryocytes in human BM cytospins and sections of bones from humanized NSGW41 and irradiated NSG mice. Scale bar, 20 μm.

(C) Expression of mCD41 and hCD61 on forward scatter low (FSC^{lo}), Ter119$^-$ CD235$^-$, h + m CD45$^-$ BM (top), and blood (bottom) cells.

(D) Frequency of human megakaryocytes (FSC^{hi} hCD45$^-$ hCD61$^+$) within all megakaryocytes (FSC^{hi}, Ter119$^-$ CD235$^-$, h + m CD45$^-$, mCD41$^+$, or hCD61$^+$) (five experiments, 2–4 mice per experiment) and frequency of human platelets within all BM (seven experiments, 1–4 mice per experiment) or blood platelets (four experiments, 1–4 mice per experiment).

(E) Human platelets in the blood of humanized NSGW41 mice 6 days after macrophage depletion (CloLip). Two experiments, 2–4 mice per experiment.

Data represent means ± SD. *p = 0.05–0.01, **p = 0.01–0.001, ***p < 0.001; n.s., not significant. See also Figure S3.

24 hr and red blood cell appearance 1–8 days after injection by flow cytometry.

EPO ELISA

Human or murine EPO levels were quantified from plasma or serum, respectively, using specific ELISAs (Quantikine; R&D Systems) according to the manufacturer's guidelines. For details on sample preparation see Supplemental Experimental Procedures.

Globin Chain Expression

For RNA isolation (RNeasy MicroKit, Qiagen) 4.4×10^4 to 8.3×10^5 hCD71$^+$ CD235$^+$ cells were sorted from BM of humanized NSG, NSGW41 and NSGW41 h*EPO*-tg mice, fresh human BM samples, or CB. cDNA was synthesized with the SuperScript First-Strand Synthesis System (Invitrogen). Semi-quantitative PCR was performed by titrating the number of amplification cycles. Primer sequences and number of amplification cycles are provided in Supplemental Experimental Procedures.

Immunohistochemistry

Fifteen weeks after humanization, cryosections from humeri were cut (3 μm) from paraformaldehyde-fixed, decalcified bones on a Cryotome CM1900 using the CryoJane Tape-Transfer System (Leica). Samples were analyzed by a fluorescence microscope (BZ-9000E; Keyence) and images were processed by BZ-Analyzer II software (Keyence) or Adobe Photoshop CS5 (Adobe). Details regarding antibodies can be found in Supplemental Experimental Procedures.

Statistical Analysis

Two-tailed Student's t tests were performed for all statistical analyses using Prism 5 for MacOSX software. In all graphs *p = 0.05–0.01, **p = 0.01–0.001, and ***p < 0.001; data represent the mean ± SD.

SUPPLEMENTAL INFORMATION

Supplemental Information includes Supplemental Experimental Procedures and three figures and can be found with this article online at http://dx.doi.org/10.1016/j.stemcr.2016.08.005.

AUTHOR CONTRIBUTIONS

S.R. designed and performed experiments, interpreted the data, and wrote the paper. R.K.W., N.K., and T.T. performed the enucleation assay and provided crucial help for morphological analysis, colony assay, and globin chain detection. J.F. performed immunohistology. A.N. analyzed erythroblast composition. M.B., R.O., and A.P. provided human cells. M.G. provided h*EPO*-tg (Tg6) mice and helped to write the manuscript. C.W. conceived the study, designed experiments, interpreted data, and wrote the paper.

ACKNOWLEDGMENTS

REFERENCES

An, X., Schulz, V.P., Li, J., Wu, K., Liu, J., Xue, F., Hu, J., Mohandas, N., and Gallagher, P.G. (2014). Global transcriptome analyses of human and murine terminal erythroid differentiation. Blood *123*, 3466–3477.

Bauer, D.E., and Orkin, S.H. (2011). Update on fetal hemoglobin gene regulation in hemoglobinopathies. Curr. Opin. Pediatr. *23*, 1–8.

Chen, Q., Khoury, M., and Chen, J. (2009). Expression of human cytokines dramatically improves reconstitution of specific human-blood lineage cells in humanized mice. Proc. Natl. Acad. Sci. USA *106*, 21783–21788.

Cosgun, K.N., Rahmig, S., Mende, N., Reinke, S., Hauber, I., Schafer, C., Petzold, A., Weisbach, H., Heidkamp, G., Purbojo, A., et al. (2014). Kit regulates HSC engraftment across the human-mouse species barrier. Cell Stem Cell *15*, 227–238.

Dzierzak, E., and Philipsen, S. (2013). Erythropoiesis: development and differentiation. Cold Spring Harb. Perspect. Med. *3*, a011601.

Geissler, E.N., McFarland, E.C., and Russell, E.S. (1981). Analysis of pleiotropism at the dominant white-spotting (W) locus of the house mouse: a description of ten new W alleles. Genetics *97*, 337–361.

Giarratana, M.C., Rouard, H., Dumont, A., Kiger, L., Safeukui, I., Le Pennec, P.Y., Francois, S., Trugnan, G., Peyrard, T., Marie, T., et al. (2011). Proof of principle for transfusion of in vitro-generated red blood cells. Blood *118*, 5071–5079.

Hu, Z., and Yang, Y.G. (2012). Full reconstitution of human platelets in humanized mice after macrophage depletion. Blood *120*, 1713–1716.

Hu, Z., Van Rooijen, N., and Yang, Y.G. (2011). Macrophages prevent human red blood cell reconstitution in immunodeficient mice. Blood *118*, 5938–5946.

Karagiannis, P., and Eto, K. (2015). Manipulating megakaryocytes to manufacture platelets ex vivo. J. Thromb. Haemost. *13* (*Suppl 1*), S47–S53.

Kaushansky, K. (2006). Lineage-specific hematopoietic growth factors. N. Engl. J. Med. *354*, 2034–2045.

Lambert, M.P., Sullivan, S.K., Fuentes, R., French, D.L., and Poncz, M. (2013). Challenges and promises for the development of donor-independent platelet transfusions. Blood *121*, 3319–3324.

Massberg, S., Brand, K., Gruner, S., Page, S., Muller, E., Muller, I., Bergmeier, W., Richter, T., Lorenz, M., Konrad, I., et al. (2002). A critical role of platelet adhesion in the initiation of atherosclerotic lesion formation. J. Exp. Med. *196*, 887–896.

Mende, N., Kuchen, E.E., Lesche, M., Grinenko, T., Kokkaliaris, K.D., Hanenberg, H., Lindemann, D., Dahl, A., Platz, A., Hofer,

T., et al. (2015). CCND1-CDK4-mediated cell cycle progression provides a competitive advantage for human hematopoietic stem cells in vivo. J. Exp. Med. *212*, 1171–1183.

Mende, N., Rahmig, S., and Waskow, C. (2016). Multilineage readout after HSC expansion—erythrocytes matter. Cell Cycle *15*, 1032–1033.

Palis, J. (2014). Of mice and men. Blood *123*, 3367–3368.

Pishesha, N., Thiru, P., Shi, J., Eng, J.C., Sankaran, V.G., and Lodish, H.F. (2014). Transcriptional divergence and conservation of human and mouse erythropoiesis. Proc. Natl. Acad. Sci. USA *111*, 4103–4108.

Rahmig, S., Bornstein, S.R., Chavakis, T., Jaeckel, E., and Waskow, C. (2015). Humanized mouse models for type 1 diabetes including pancreatic islet transplantation. Horm. Metab. Res. *47*, 43–47.

Rongvaux, A., Willinger, T., Takizawa, H., Rathinam, C., Auerbach, W., Murphy, A.J., Valenzuela, D.M., Yancopoulos, G.D., Eynon, E.E., Stevens, S., et al. (2011). Human thrombopoietin knockin mice efficiently support human hematopoiesis in vivo. Proc. Natl. Acad. Sci. USA *108*, 2378–2383.

Rongvaux, A., Willinger, T., Martinek, J., Strowig, T., Gearty, S.V., Teichmann, L.L., Saito, Y., Marches, F., Halene, S., Palucka, A.K., et al. (2014). Development and function of human innate immune cells in a humanized mouse model. Nat. Biotechnol. *32*, 364–372.

Sharma, Y., Astle, C.M., and Harrison, D.E. (2007). Heterozygous kit mutants with little or no apparent anemia exhibit large defects in overall hematopoietic stem cell function. Exp. Hematol. *35*, 214–220.

Suzuki, K., Hiramatsu, H., Fukushima-Shintani, M., Heike, T., and Nakahata, T. (2007). Efficient assay for evaluating human thrombopoiesis using NOD/SCID mice transplanted with cord blood CD34+ cells. Eur. J. Haematol. *78*, 123–130.

Vogel, J., and Gassmann, M. (2011). Erythropoietic and non-erythropoietic functions of erythropoietin in mouse models. J. Physiol. *589*, 1259–1264.

Waskow, C., Paul, S., Haller, C., Gassmann, M., and Rodewald, H. (2002). Viable c-Kit(W/W) mutants reveal pivotal role for c-kit in the maintenance of lymphopoiesis. Immunity *17*, 277–288.

Waskow, C., Terszowski, G., Costa, C., Gassmann, M., and Rodewald, H.R. (2004). Rescue of lethal c-KitW/W mice by erythropoietin. Blood *104*, 1688–1695.

Supplemental Information

Improved Human Erythropoiesis and Platelet Formation in Humanized NSGW41 Mice

Susann Rahmig, Romy Kronstein-Wiedemann, Juliane Fohgrub, Nicole Kronstein, Aleksandra Nevmerzhitskaya, Martin Bornhäuser, Max Gassmann, Alexander Platz, Rainer Ordemann, Torsten Tonn, and Claudia Waskow
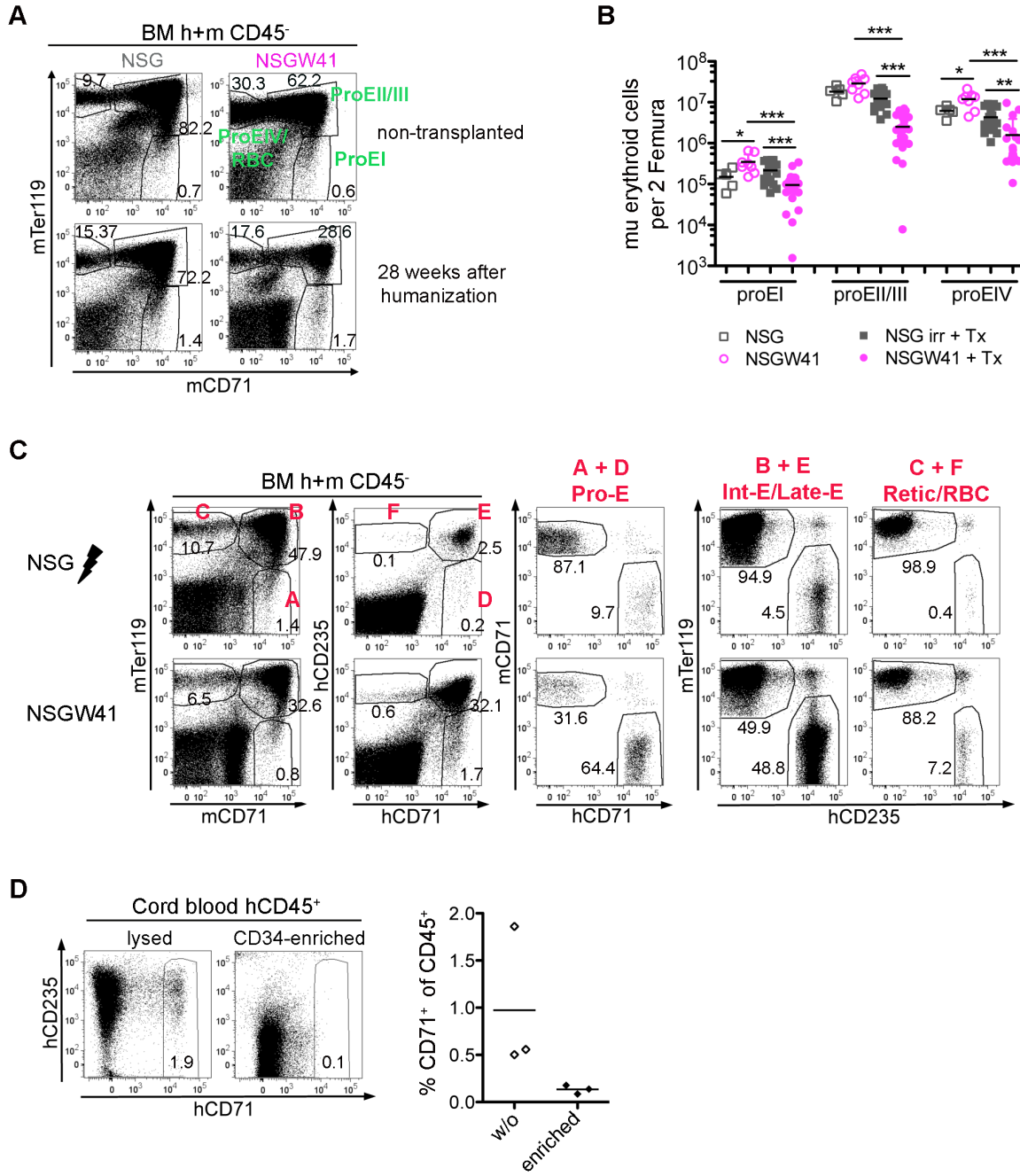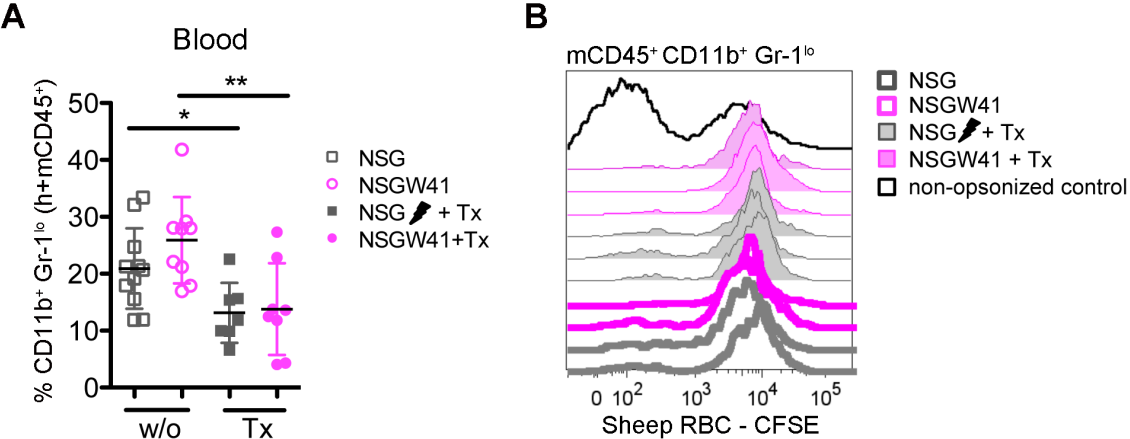
Figure S1:

A

BM h+m CD45⁻

NSG   NSGW41

mTer119

9.7 / 82.2 / 0.7

30.3 / 62.2 / 0.6 — ProEII/III, ProEIV/RBC, ProEI

non-transplanted

15.37 / 72.2 / 1.4

17.6 / 28.6 / 1.7

28 weeks after humanization

mCD71

B

mu erythroid cells per 2 Femura

*** over proEI
*** / *
*** over proEII/III ***
*** / * / ** over proEIV

proEI   proEII/III   proEIV

□ NSG   ■ NSG irr + Tx
○ NSGW41   ● NSGW41 + Tx

C

BM h+m CD45⁻

A + D Pro-E   B + E Int-E/Late-E   C + F Retic/RBC

NSG ⚡
mTer119
C 10.7 / B 47.9 / A 1.4
F 0.1 / E 2.5 / D 0.2
mCD71: 87.1 / 9.7
94.9 / 4.5
98.9 / 0.4

NSGW41
6.5 / 32.6 / 0.8
0.6 / 32.1 / 1.7
31.6 / 64.4
49.9 / 48.8
88.2 / 7.2

mCD71   hCD71   hCD71   hCD235   hCD235

hCD235 / hCD71 (axes)
mCD71 (axis)
mTer119 (axis)

D

Cord blood hCD45⁺

lysed   CD34-enriched

hCD235

1.9   0.1

hCD71

% CD71⁺ of CD45⁺

w/o   enriched

Figure S2:

A

Blood

% CD11b⁺ Gr-1ˡᵒ (h+mCD45⁺)

$*$

$**$

□ NSG
○ NSGW41
■ NSG⚡ + Tx
● NSGW41+Tx

w/o   Tx

B

mCD45⁺ CD11b⁺ Gr-1ˡᵒ

□ NSG
□ NSGW41
□ NSG⚡+ Tx
□ NSGW41 + Tx
□ non-opsonized control

Sheep RBC - CFSE
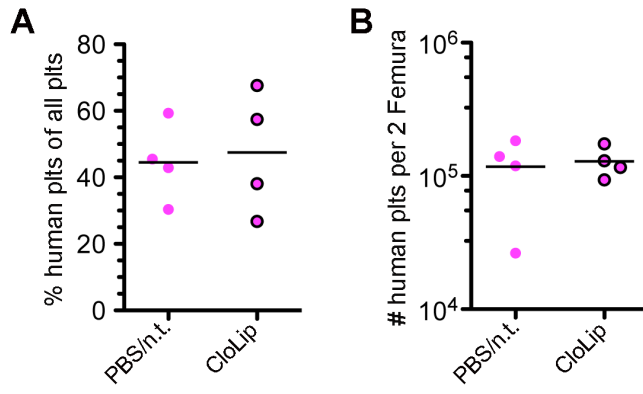
Figure S3:

Figure S1. Analysis of murine and human erythroid progenitors in humanized mice by flow cytometry, Related to Figure 1
(A) Dot plots show the expression of Ter119 and mCD71 on CD45$^-$ (human and mouse) bone marrow cells of humanized NSG and NSGW41 mice. (B) Total numbers of murine RBC differentiation stages in 2 femura of non-transplanted and humanized NSG and NSGW41 mice. 6 expts, 2-9 mice each per expt. Depicted are mean ± SD. (C) Gating strategies to determine the relative contribution of human donor cells to the indicated erythroid progenitor compartments. (D) Dot plots (left) and graph (right) show the presence of CD71$^+$ erythroid progenitors within ACK-lysed or CD34-enriched human cord blood (2 expts).

Figure S2. Murine macrophages in humanized NSG and NSGW41 mice, Related to Figure 3
(A) Plot shows the frequency of CD11b$^+$ Gr-1^{lo} macrophages in the blood of humanized or non-humanized NSG or NSGW41 mice. Mice had received human CD34-enriched CB cells 11-21 weeks before. 3 expts, 2-4 mice each per expt. Depicted are mean ± SD. (B) Phagocytic activity of murine blood macrophages from indicated mouse strains before and after humanization.

Figure S3. Human thrombocytes in bone marrow after CloLip treatment, Related to Figure 4
NSGW41 mice were injected with 200µl clodronate liposomes (CloLip) to deplete macrophages 11 weeks after humanization. (A) Frequency of human platelets within all platelets in bone marrow of CloLip- or PBS-treated NSGW41 mice. (B) Total numbers of human platelets in 2 femura of CloLip- or PBS-treated NSGW41 mice. 1 expt, 4 mice each. Depicted are mean ± SD.

Supplemental Experimental Procedures

Genotyping of NSGW41 mice

Genotyping of Kit^{W41} allele was performed by PCR on tail-snip DNA (forward: 5'-AAGGAAGGTTAGAACCCCTGG; reverse: 5'- AGCTCCCAGAGGAAATCCC). The products were sequenced using the forward primer. The Kit^{W41} allele contains a point mutation at position 2519 (G / A) (Nocka et al., 1990).

Antibodies

Human cells were stained using antibodies specific for (clone names given in brackets): CD3 (OKT3), CD19 (HIB19), CD33 (WM-53), CD42a (GR-P), CD45 (HI30), CD235 (HIR2) from eBioscience, CD45 (HI30), CD16 (3G8), CD41 (HIP8), CD61 (VI-PL2) from Biolegend, CD14 (M5E2) (BD Biosciences) and CD71 (MEM-75) from ImmunoTools. Murine cells were stained with the following antibodies: CD11b (M1/70), CD41 (eBioMWReg30), CD45 (30-F11), CD115 (AFS98), Gr-1 (RB6-8C5), Ly-6C (HK1.4), Ter119 (TER-119) (all from eBioscience), CD41 (MWReg30) and CD71 (C2) from BD Biosciences. Blocking reagents used were ChromPure mouse IgG (Jackson ImmunoResearch) for human cells and rat IgG (Dianova) as well as anti-mouse CD16/CD32 (93) (eBioscience) for murine cells. For immunohistochemistry sections were blocked with rat Ig (500 µg/ml, Jackson ImmunoResearch Laboratories) and Streptavidin/Biotin blocking kit (Vector Laboratories). Antibodies used for immunostaining were hCD45 (HI30), mCD45 (30-F11), hCD42a (GR-P) and mCD41 (MWReg30) (eBioscience). Anti-FITC-Alexa488 (Molecular Probes) and streptavidin-Cy3 (Jackson ImmunoResearch Laboratories) were used for secondary steps. Dapi (2 µg/ml) was used to stain nuclei.

EPO ELISA

Samples were collected into EDTA containing micro tubes (plasma) or non-coated tubes (serum) and centrifuged at 2000g for 15 minutes at RT. Plasma samples from NSGW41 h*EPO*-tg mice were diluted 2- to 10-fold. All serum samples were diluted 1:2 before use. The optical density was measured on a Sunrise™ absorbance reader (Tecan). A standard curve was generated using nonlinear regression.

May-Gruenwald-Giemsa staining

May-Gruenwald-Giemsa staining was modified from Waskow et al., 2008. In brief, cytospins were stained in 100% and 50% May-Gruenwald solution (Merck, Darmstadt, Germany) for 3 minutes each. After rinsing in water (pH6.8) for 2 minutes the slides were stained in Giemsa (Merck, Darmstadt, Germany) for 15 minutes. Samples were then washed in water (pH6.8) for 3 minutes and quickly rinsed with ethanol and water to remove excessive dye. Slides were air-dried before microscopy.

Primers for globin chain expression

α-globin (NM_000558.4): f: 5'- CTGGAGAGGATGTTCCTGTCCTTG, r: 5'- CAGCTTAACGG TATTTG GAGGTCAT (t_A=59 °C; 24/26/28/30 cycles)

β-globin (NM_000518.4): f: 5'- TCCTGAGGAGAAGTCTGCCGTTAT, r: 5'- GAAATTGGACAG CAAGA AAGCGGA (t_A=53 °C; 26/28/30/32 cycles)

γ-globin (NM_000559.2): f: 5'- ACTCGCTTCTGGAACGTCTGA, r: 5'- GTATCTGGAGGAC AGGGCA CT (t_A=57 °C; 24/26/28/30 cycles)

δ-globin (NM_000519.3): f: 5'-GCAGATTACTGGTGGTCTACCCTTG, r: 5'- GGAAACAGTCC AGGAT CTCAAT GG (t_A=55 °C; 26/28/30/32 cycles)

β-actin (NM_001101.3): f: 5'- AGCGAGCATCCCCCAAAGTT, r: 5'- GGGCACGAAGGCTCAT CATT (t_A=59 °C; 28/30/32/34 cycles)

Phagocytosis assay

3ml defibrinated sheep red blood cells (sRBC, Thermo Scientific) were opsonized in 10ml PBS/1% BSA containing 100µg/ml rabbit IgG specific for sRBC (MP Biomedicals) for 30' at 37°C and 30' on ice and subsequently labeled ($4*10^7$ sRBCs/ml) with CFSE at a final concentration of 5µM. WBCs from lysed blood of non-transplanted and humanized (21 weeks post Tx) NSG and NSGW41 mice were incubated with opsonized CFSE-labeled sheep RBCs in a ratio of 1:100 for 4h at 37°C. Subsequently, sheep RBCs were lysed in ACK buffer for 1min, cells were stained and analyzed by

flow cytometry. Non-opsonized sRBCs were used as control, and non-engulfed sheep RBCs sticking to WBCs were excluded by gating on PE anti-rabbit IgG negative cells.

Supplemental References

Nocka, K., Tan, J.C., Chiu, E., Chu, T.Y., Ray, P., Traktman, P., and Besmer, P. (1990). Molecular bases of dominant negative and loss of function mutations at the murine c-kit/white spotting locus: W37, Wv, W41 and W. The EMBO journal *9*, 1805-1813.

Waskow, C., Liu, K., Darrasse-Jeze, G., Guermonprez, P., Ginhoux, F., Merad, M., Shengelia, T., Yao, K., and Nussenzweig, M. (2008). The receptor tyrosine kinase Flt3 is required for dendritic cell development in peripheral lymphoid tissues. Nature immunology *9*, 676-683.